

## Fractal Dimensions of Martensitic Microstructures

E. Hornbogen, Institut für Werkstoffe, Ruhr-Universität, Bochum, FRG

The feasibility of the application of the geometry of non-integer dimensions to martensitic microstructures is discussed. Microscopic analysis reveals the following phenomena:

1. There is non-fractal and fractal martensite
2. Fractal martensite implies  $x \geq 3$  subsequent fragmentations of an austenite grain
3. For metallographic sections the following aspects can be described by fractal functions:
  - a) volume fractions of martensite,
  - b) density and ruggedness of martensite-austenite interfaces,
  - c) size distribution of martensite crystals,
  - d) local distribution of residual austenite,
  - e) roughness of fracture surfaces of martensite.

Simple geometrical models are proposed which demonstrate essential features of fractal martensite. The relevance for materials properties such as toughness or shape memory are briefly discussed.



The concepts of Euclidian geometry imply integer dimensions  $d$ , which control scaling laws. They are used for the characterization of microstructural elements in solids and range between  $0 \leq d \leq 3$  (1):

- $d = 0$  point defects, solute atoms,
- $d = 1$  dislocations,
- $d = 2$  grain boundaries, interfaces, surfaces,
- $d = 3$  dispersed particles and pores.

Classical geometry has recently been extended to non-integer dimensions  $D > d$  for the description of structures with a certain type of disorder, which is characterized by multiple branching, rugged lines and surfaces, uneven distribution of spacings, diameters or steps (2). Such features are more common in nature than ideal Euclidian shapes (3). Martensitic transformation of austenite provides a good example for the application of this new geometry (4). In this paper several simple models are proposed which simulate typical features of martensitic microstructures (Fig. 1).

The fractal dimension can be calculated from the geometrical type of the motive. It may consist of  $N$  segments. The original size ( $L_0$  for a line) is subdivided by a factor  $1/n$  for each iteration  $x$ :  $n^x = \epsilon$ . Therefore, the total length of a line increases to  $L_{(x+1)} > L_x$ :

$$L_{(x+1)} = L_x N \cdot n \quad \text{Equ. 1}$$

$$D = \frac{\log N}{\log \frac{1}{n}} \geq 1 \quad \text{Equ. 2}$$

Correspondingly, for  $D > 1$  the measured length of a line depends on the scale of the yardstick  $\epsilon$  which is used for its (metallographic) analysis:

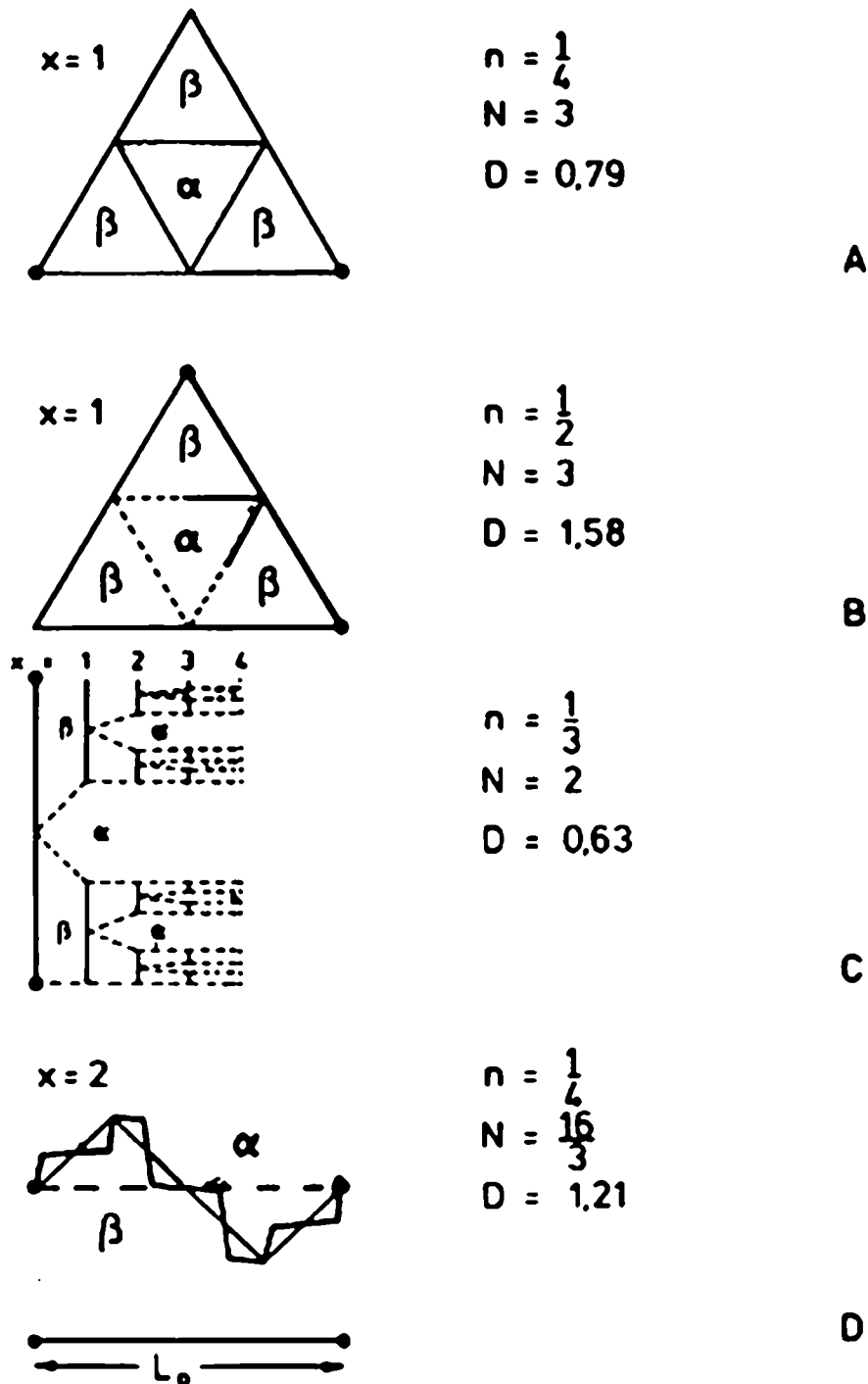


**Fig. 1:** Geometrical models for aspects of martensitic microstructures,  $x$  = number of self-similar fragmentations (metallographic sections). A) Sierpinski-triangle, volume fractions of martensite  $\alpha$  in austenite  $\beta$ , subdivision of austenite grain; B) Formation of  $\beta/\alpha$ -interfaces; C) Cantor-bar, formation of a spectrum of sizes of martensite  $\alpha$  and spacings of residual austenite  $\beta$  (compare fig. 5); D) roughening of a line (i. e.  $\beta/\alpha$  interface or fracture surface)

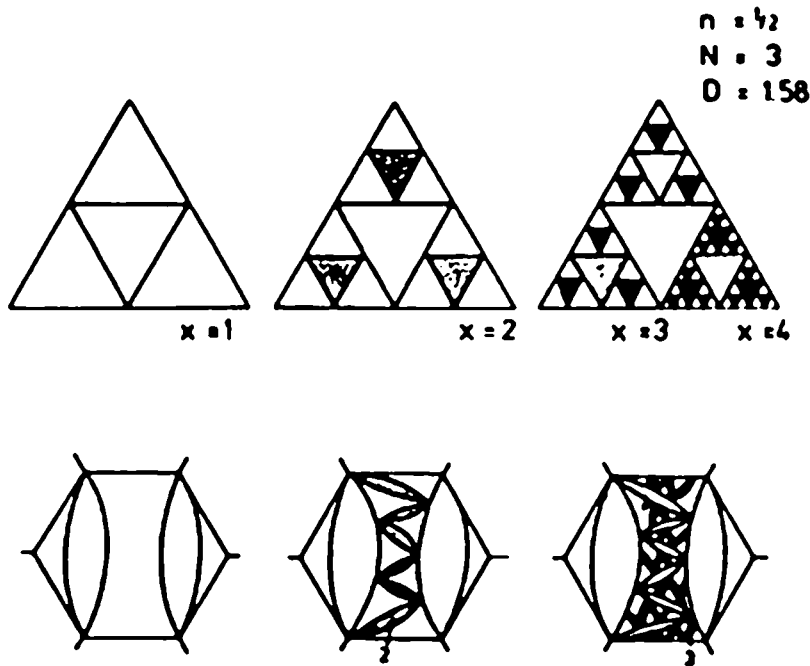


**Fig. 2:** Subsequent formation of  $x$  generations of martensite, schematic

$$L_{\epsilon} = L_0 \epsilon^{d-D} = L_0 \epsilon^{1-D} \quad \text{Equ. 3}$$

$$\epsilon = \frac{r}{L_0 M} \quad \text{Equ. 4}$$

$M$  is the magnification and  $r$  the resolution or the radius of a circle which is used to probe the length of a line  $L_{\epsilon}$ .

Figure 1 summarizes geometrical motives which have been proposed to simulate the following features of a martensitic transformation:

- A. The area in a micrograph (volume fraction  $f_{\alpha}$ ) of martensite which forms by subsequent fragmentations  $x$  in an austenite grain (size  $L_0$ )
- B. The density of austenite/martensite ( $\beta/\alpha$ ) interfaces which form simultaneously
- C. The sizes of martensite crystals and the spacings between "particles" of residual austenite
- D. The true boundary area for the case of rugged interfaces.

Figure 2 provides schematic drawings of the features which resemble more closely the real microstructures shown in figure 3. Metallographic sections of two-dimensional microstructural elements (interfaces) become lines in the metallographic analysis ( $D \geq 1$ ). An evaluation of measured volume fractions  $f_{\alpha}$  of martensite produced by subsequent fragmentation  $x = 3$  of austenite grains ( $f_{\beta} = 1 - f_{\alpha}$ ) is shown in figure 4.

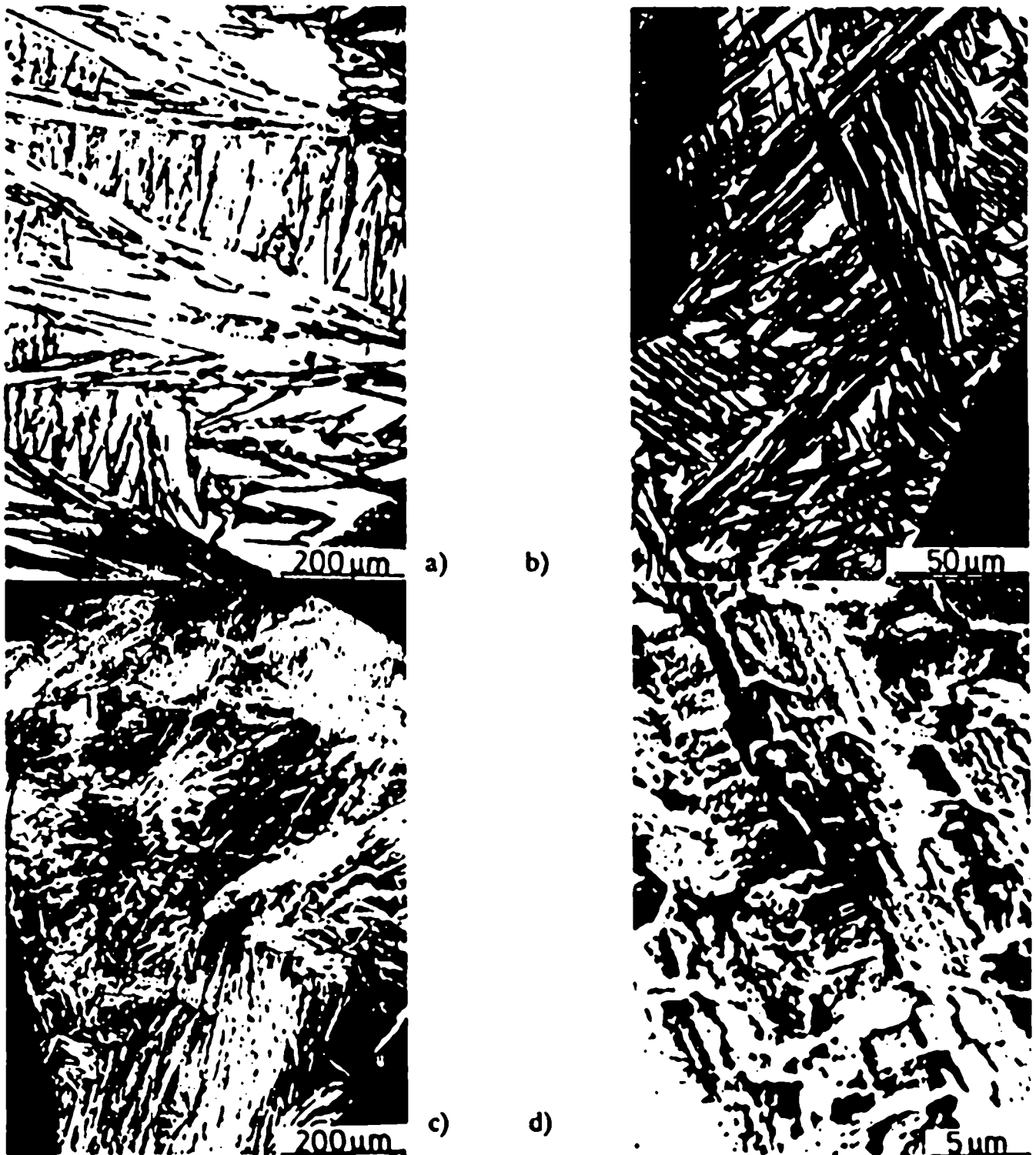


Fig. 3:

Microscopy of fractal microstructures

- A) FeNi<sub>31.4</sub>-Al<sub>4.2</sub> (wt%) cooled to  $-190^{\circ}\text{C}$ ,  $x = 3$  fragmentations are visible
- B) FeNi<sub>26.5</sub>-Al<sub>5.9</sub> (wt%) aged 1 h  $500^{\circ}\text{C}$  before due to interaction with dispersed particles in austenite, rugged interfaces
- C) FeNi<sub>31.4</sub>-4,2Al (wt%) 75 % plastic deformation before transformation, "chaotic" martensite (N. Jost)
- D) CuAlNiMnTi shape memory alloy, embrittled by ageing 20 h  $200^{\circ}\text{C}$ , fractal fracture surface by multiple cleavage at martensite grain and variant boundaries in addition to intra martensitic fracture (E. Kobus)

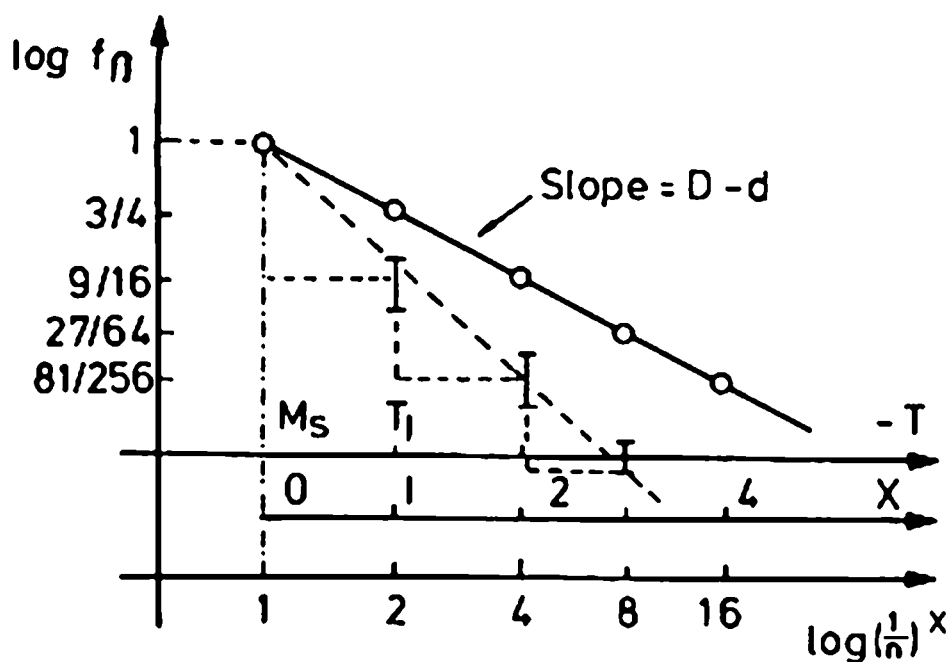


Fig. 4: Calculated data for fragmentation of Sierpinski-triangle and metallographic measurements for partially transformed FeNi<sub>31.4</sub>-Al<sub>4.2</sub> alloy (see fig. 3)

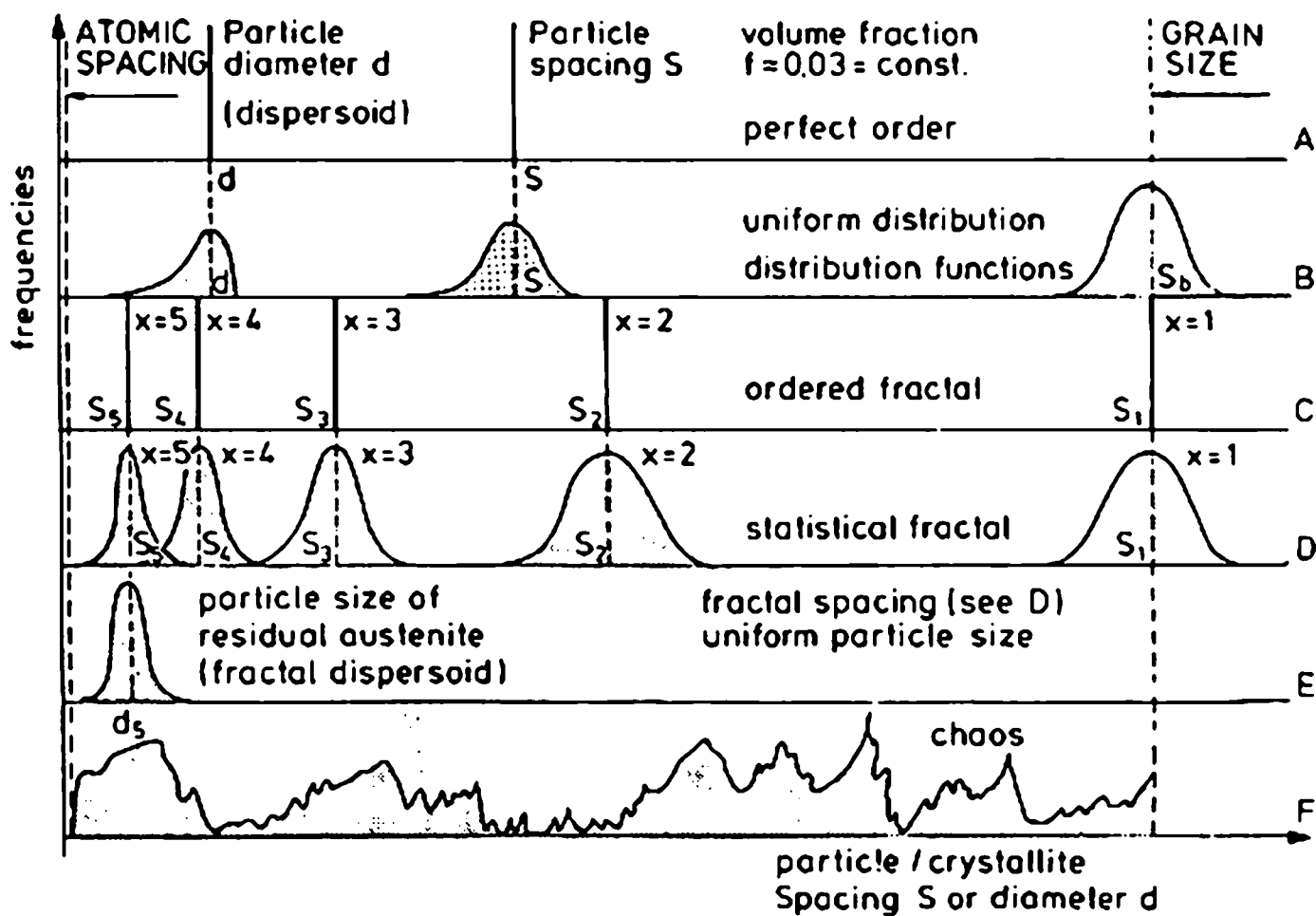
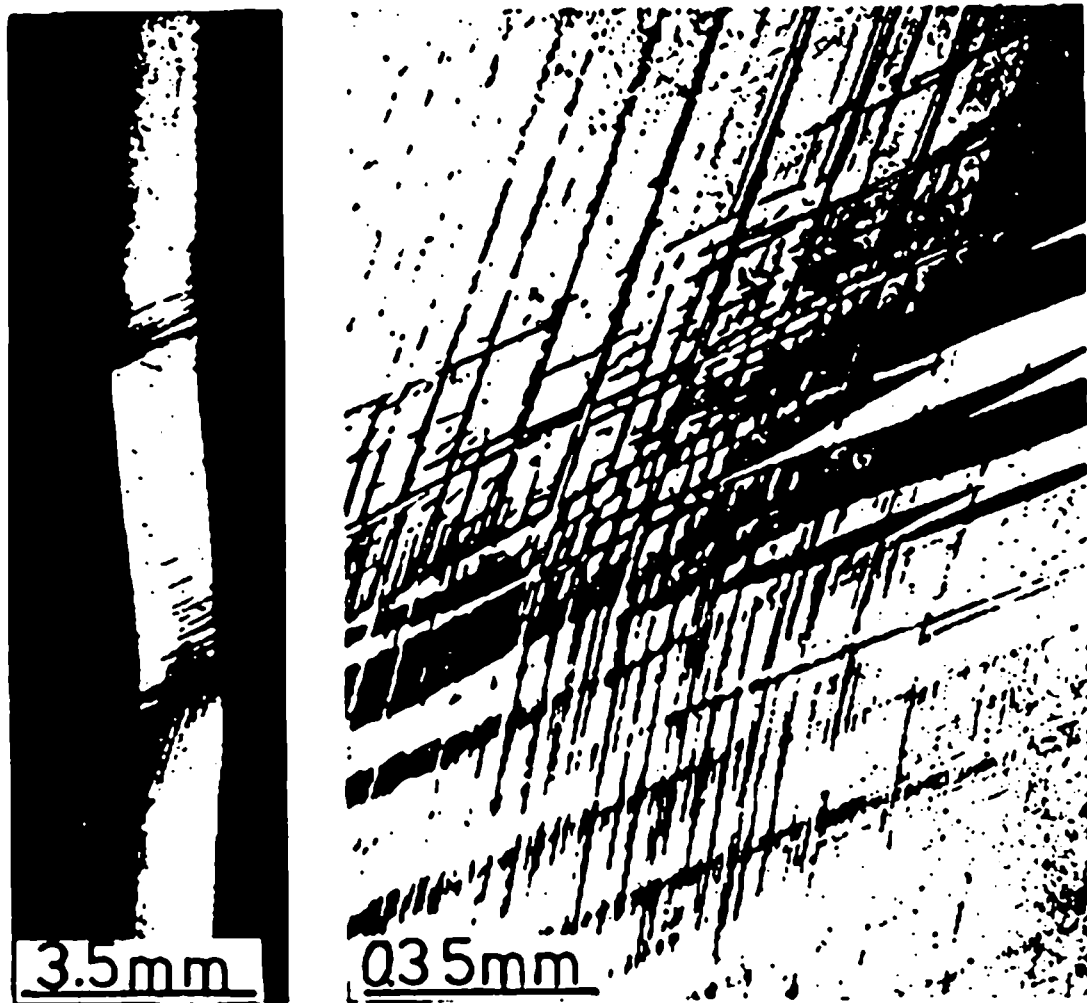


Fig. 5: Microstructural parameters for different types of dispersion structures  
 A, B) Complete order, disorder due to scatter around average: classical microstructures  
 C, D, E) Spectrum of discrete sizes, scatter around spectral sizes: fractal microstructures  
 F) Chaotic microstructure



**Fig. 6:** Example for non-fractal martensite, formation of an  $\alpha$ -single-crystal from a  $\beta$ -CuZn 40 (wt%) single crystal by shear stress.

Figure 5 explains in a systematic way the special characteristics of a fractal martensitic microstructure which are found between microstructural order and chaos. An ordered microstructure implies discrete values for particle size and spacing (Fig. 5D). Usually, these parameters are relaxed by statistical functions but average values can still be determined. The microstructure of fractal martensite consists of a spectrum of size of lenticular martensite crystals. These sizes correspond to the spacings between "particles" of residual austenite. It does not form a classical but a fractal dispersion. Microstructural chaos is defined by the impossibility to determine any average values or spectra of sizes or spacings of microstructural elements (Fig. 5F).

There are fractal and non-fractal martensitic microstructures. An example is shown in Fig. 6: the transformation of austenite by an external shear stress which activates only one crystallographic variant of martensite. This definitely produces a non-fractal structure.

There are the following prerequisites for the formation of fractal martensite:

- a. independent formation of more than one crystallographic variant,
- b. limited side-wise growth of lenticular or plate-shaped crystals,
- c. ability of the  $\beta/\alpha$ -interface to act as nucleation site for subsequent fragmentations.

Formation of rough  $\beta/\alpha$  interfaces is favoured by the presence of defects (5) or particles (6,7) in the austenite before transformation. Favourable conditions for the formation of fractal martensite are provided by coarse-grained alloys of iron of relatively high yield stress and a sufficiently high  $M_s$ -temperature, to allow for several fragmentations.

Embrittled fractal martensite shows a fractal fracture surface. It is due to crack paths along phase and variant boundaries in addition to transmartensitic cracking. This provides a special case where the claims of fractal fracture (8) are justified (Fig. 3D). Fracture surfaces of materials with other microstructures are often non-fractal (3).

Fractal martensite will form in more or less discrete steps. The analysis of the  $f_\alpha(\Delta T)$ -functions (amount of martensite vs undercooling  $M_s - T = \Delta T$ ) should be aided by consideration of the fractal nature of its origin. The relation between the sequence of  $x$  fragmentations and temperature  $T < M_s$  is still to be explored.

The degree of fractality (i. e. number of recognizable generations  $x \leq 3$ ) is less pronounced in shape memory alloys (TiNi-, CuZn-base). This is due to the high mobility of the  $\beta/\alpha$ -interface in connection with minimum volume change. It leads to the formation of packages of orientational variants by side-wise growth which is not a self-similar microstructure.

An unexplored field are microstructure-property relations of fractal structures. For ferrous alloys two-phase aggregates of a hard and brittle phase (martensite) form in more ductile austenite with a fractal local distribution. Percolation (i. e. a net) instead of dispersion of the brittle phase explains the unfavourable mechanical properties often found in such microstructures. BCC shape memory alloys should show the inverse behaviour: a softer phase forms in a harder matrix. Steppyness of forces exerted by shape-memory actuators may be caused by fractal formation of martensite and austenite. The effects of fractality of martensite on bulk properties may provide a field for fruitful future research.

### Acknowledgement

This work is supported by the Volkswagen Foundation (Project COSMOS I/63846).

**References:**

- (1) E. Hornbogen: *J. Mat. Sci.* **21** (1986), 3737
- (2) B. B. Mandelbrot: *The Fractal Geometry of Nature*, 1983, New York, W. H. Freeman
- (3) E. Hornbogen: *Int. Mat. Rev.* **34** (1989)
- (4) E. Hornbogen: *Z. Metallkde* **78** (1987) 352
- (5) N. Jost, E. Hornbogen: *J. Mat. Sci. Lett.* **6** (1987) 491
- (6) H. J. Neuhauser, W. Pitch: *Acta Met.* **19** (1970) 337
- (7) E. Hornbogen: *Martensitic Transformations (ICOMAT-86)*, 1986, Jap. Inst. Metals, Sendai, 453
- (8) B. B. Mandelbrot, D. Passoja: *Nature* **308** (1984) 771